

Design of the Advanced LIGO Recycling Cavities

Muzammil A. Arain* and Guido Mueller

Department of Physics, University of Florida, Gainesville, FL, 32611-8440, USA

*Corresponding author: muzamil@phys.ufl.edu

Abstract: The current LIGO detectors will undergo an upgrade which is expected to improve their sensitivity and bandwidth significantly. These advanced detectors are likely to employ stable recycling cavities to better confine their spatial eigenmodes instead of the currently installed marginally stable power recycling cavity. In this letter we describe the general layout of the recycling cavities and give specific values for a first possible design. We also address the issue of mode mismatch due to manufacturing tolerance of optical elements and present a passive compensation scheme based upon optimizing the distances between optical elements.

©2008 Optical Society of America

OCIS codes: (120) Instrumentation, measurement, and metrology; (120.2230) Fabry-Perot; (120.3180) Interferometry; (350.1260) Astronomical Optics; (350.4600) Optical Engineering.

References and links

1. S. J. Waldman *et al*, "Status of LIGO at the start of the fifth science run," *Class. Quantum Grav.* **23**, S653-S660 (2006).
2. R. Adhikari, P. Fritschel, and S. Waldman, "Enhanced LIGO," LIGO Technical Note LIGO-T060156-01-I, <http://www.ligo.caltech.edu/docs/T/T060156-01.pdf>.
3. A. Weinstein, "Advanced LIGO optical configuration and prototyping effort," *Class. Quantum Grav.* **19**, 1575-1584 (2002).
4. C. Wilkinson, "Plans for Advanced LIGO Instruments," presented at the 2005 APS April Meeting, Tampa, Florida, USA, 16-19 April 2005.
5. A. M. Gretarsson, E. D'Ambrosio, V. Frolov, B. O'Reilly, and P. K. Fritschel, "Effects of mode degeneracy in the LIGO Livingston Observatory recycling cavity," *J. Opt. Soc. Am. B* **24**, 2821-2828 (2007).
6. G. Mueller, "Stable Recycling Cavities for Advanced LIGO," LIGO document LIGO-G050423-00-Z, <http://www.ligo.caltech.edu/docs/G/G050423-00/G050423-00.pdf>.
7. M. A. Arain, "Thermal Compensation in Stable Recycling Cavity," presented at the LSC March meeting, Louisiana, USA, March 2006, <http://www.ligo.caltech.edu/docs/G/G060155-00/G060155-00.pdf>.
8. G. Mueller, "Stable recycling cavities for Advanced LIGO," presented at the LIGO-Virgo meeting, Hannover, Germany, October 2007, available at www.ligo.caltech.edu/docs/G/G070691-00.pdf.
9. G. Mueller, "Beam jitter coupling in advanced LIGO," *Opt. Express* **13**, 7118-7132 (2005), <http://www.opticsinfobase.org/abstract.cfm?URI=oe-13-18-7118>.
10. N. Mavalvala, D. Sigg, and D. Shoemaker, "Experimental Test of an Alignment-Sensing Scheme for a Gravitational-Wave Interferometer," *Appl. Opt.* **37**, 7743-7746 (1998).
11. Y. Pan, "Optimal degeneracy for the signal-recycling cavity in advanced LIGO," manuscript submitted for publication, http://arxiv.org/PS_cache/gr-qc/pdf/0608/0608128v1.pdf.
12. G. Heinzel *et al*, "Dual recycling for GEO 600," *Class. Quantum Grav.* **19**, 1547-1553 (2002).
13. F. Acernese *et al*, "Status of Virgo," *Class. Quantum Grav.* **22**, S869-S880 (2002).
14. R. Takahashi *et al*, "Status of TAMA300," *Class. Quantum Grav.* **22**, S403-S408 (2004).
15. P. Fritschel, "Second generation instruments for the Laser Interferometer Gravitational Wave Observatory (LIGO)," *Proc. SPIE* **4856**, 282-291 (2003).
16. G. Mueller, "Parametric Instabilities and the geometry of the recycling cavities," presented at the Parametric Instability Workshop, Perth, Australia, 16-18 July, 2007, www.ligo.caltech.edu/docs/G/G070441-00.pdf.
17. R. Lawrence, "Active Wavefront Correction in Laser Interferometric Gravitational Wave Detectors," PhD Dissertation, Massachusetts Institute of Technology, (2003).

1. Introduction

The Laser Interferometer Gravitational Wave Observatory (LIGO) just finished its fifth science run [1]. The LIGO Science Collaboration (LSC) is currently analyzing the data while the detectors are being upgraded. This upgrade will improve the sensitivity by an additional factor of two to three and will lead to a new year-long science run that will start in the fall of 2008 [2]. After that science run virtually all components of the current detectors will be replaced, the optical configuration will change, and the laser power will be increased [3,4]. Once Advanced LIGO has been commissioned, the sensitivity will be improved by another order of magnitude.

In addition to power recycling, Advanced LIGO will employ signal recycling, a technique which allows to tune the frequency response of the detector. The current baseline design of Advanced LIGO carries a design for the recycling cavities (RCs) that is similar to the design of the power recycling cavity (PRC) in the current LIGO detector. This design employs a PRC which is optically equivalent to a cavity with essentially flat mirrors; the effective radii of curvatures (ROCs) and the subsequent Rayleigh range of the spatial cavity eigenmode are large compared to the distance between the mirrors. This leads to a marginally stable cavity (MSC). Consequently, the transversal mode spacing inside the MSC is well below the linewidth of the RC. This has led to significant problems during the commissioning phase of LIGO [5].

In this letter we will present an alternative design which is commonly known as a Stable Recycling Cavity: a cavity with a transversal mode spacing that is much larger than the linewidth of the RCs [6-8]. Note that we can have a stable PRC as well as stable signal recycling cavity (SRC). This has far reaching consequences for many other effects and subsystems. Alignment sensing signals, parametric instabilities, decreased losses in the gravitational wave signals, and changes in the coupling of beam jitter into the gravitational wave channel are among the most prominent areas which are affected [9-11]. It should be noted that signal recycling has been tested at the GEO detector [12], various table top experiments, and is currently being tested again at the 40m prototype at the California Institute of Technology. All these test interferometers employed or employ stable RCs while LIGO, VIRGO, and TAMA are using marginally stable power RCs [13,14].

In section 2, we describe the general layout of the stable RCs, discuss the design constraints, and give a first specific layout which is currently being used for detailed trade studies. In section 3, we derive first requirement on the mode matching between the RCs. Errors in the ROCs of the telescope mirrors in the RCs and the arm cavity mirrors will be discussed in section 4. Although most of the conclusions will be applicable to both RCs, some differences exist and will be discussed in the summary in section 5.

2. Advanced LIGO Optical Configuration

Advanced LIGO is a long base line dual recycled cavity enhanced Michelson interferometer (see Fig. 1) [15]. Two mirrors inside each arm of the Michelson interferometer form a cavity enhanced arm. The mirror near the beam splitter (BS) is termed as input test mass ($ITM_{x,y}$) while the second mirror placed at a distance of 4 km from the ITM is called end test mass ($ETM_{x,y}$). To increase the power inside the arm, a partially reflecting mirror called power recycling mirror (PRM) is installed at the symmetric (bright) port of the interferometer. Note that PR_1 and SR_1 will be used interchangeably for PRM and SRM respectively throughout the paper. To increase the sensitivity to the gravitational signal, a partially reflecting mirror is also installed at the anti-symmetric (dark) port of the interferometer. This mirror is termed as signal recycling mirror (SRM). Gravitational waves will change the arm length differentially and thus changes the electric field behind the SRM.

Here the carrier light (red lines in Fig. 1) are resonant every where in the interferometer, i.e., inside the two RCs and the arm cavities. There will be two pair of radio-frequency (RF) side bands to control the length and the alignment of the interferometer (indicated by green

lines). These RF sidebands are produced by the electro-optic modulators (EOMs). Both of these sidebands will be anti-resonant in the arm cavities. One RF sideband will be resonant in the PRC while the other will be resonant in both PRC and SRC. The gravitational wave signal sidebands generated via the differential motion of the two arm cavities will propagate in the SRC. The position of the signal recycling mirror (SRM) can be used to tune the frequency response of the interferometer for gravitational wave signals.

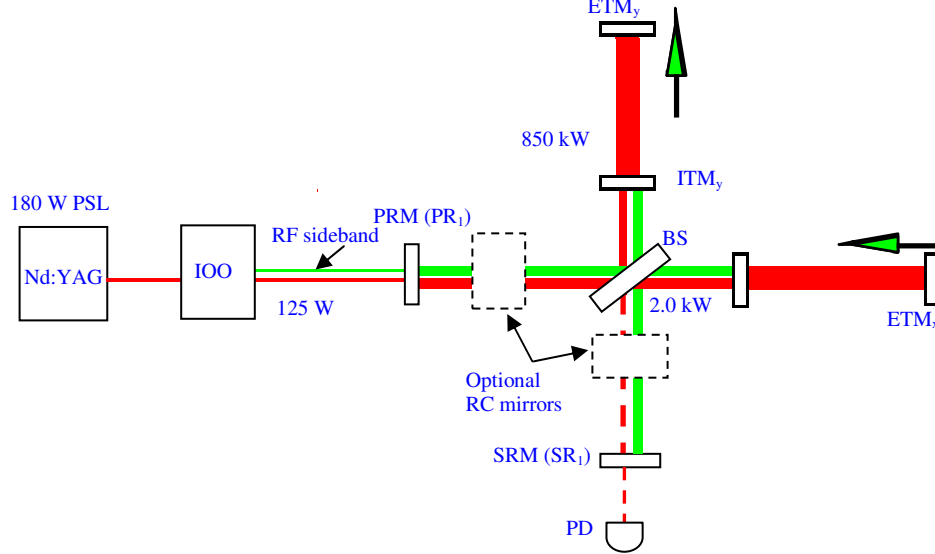


Fig. 1. Optical configuration of dual recycled cavity-enhanced Advanced LIGO detector. Here power levels at various points in the interferometer are also shown. Red lines indicate carrier electric field while the green lines show the RF sidebands produced by the electro-optic modulators in the IOO section. Here ITM: Input test mass, ETM: End test mass, BS: Beam splitter, PRM: Power recycling mirror, SRM: Signal recycling mirror, RC: Recycling cavity, PD: Photo-detector, IOO: Input output optics, and PSL: Pre-stabilized laser.

In the current design of the Advanced LIGO arm cavities the ROC of the ITMs is $R_{ITM} = 1971\text{m}$ and for the end test masses (ETMs) is $R_{ETM} = 2191\text{m}$. The beam sizes on the mirror surfaces would then be $w_{ITM} = 5.55\text{cm}$ ($1/e^2$ intensity beam radius) and $w_{ETM} = 6.2\text{cm}$. This has changed from the originally symmetric design of $R_{ITM} = R_{ETM} = 2076\text{m}$ with 6cm beam sizes to reduce diffraction losses at the beam splitter.

2.1 Design of RC

The proposed design of the arm cavities for Advanced LIGO has not changed significantly over the last years, but there is considerable discussion about the design of the RCs [11,15]. In the original baseline design, each RC was formed between the arm cavities and a single mirror. This design together with the constraints of the vacuum system leaves no freedom to choose the eigenmode parameters like the transversal mode spacing (or the Gouy phase) inside the RCs. The RCs are essentially marginally stable with a vanishing round trip Gouy phase and a transversal mode spacing that is much smaller than the linewidth of the RCs.

This design has several potential problems. For example it is very sensitive to ROC mismatches and even small mode mismatches will cause significant signal losses [11]. One way to create stable RCs starting with a 5.5cm beam size and being restricted by the vacuum envelope to distances of less than 24m is shown in Fig. 2a. The beam coming from the ITM, (for simplicity we include only one arm cavity in this discussion) of the arm cavities could be focused inside the RCs using a strong lens or curved mirror (PR_2). As we would have to focus the 5.5cm beam over this short distance, the convergence angle would be on the order of:

$$\alpha \propto \frac{5.5 \text{ cm}}{24 \text{ m}} = 2.3 \text{ mrad.} \quad (1)$$

The waist and Rayleigh range of such a beam is:

$$w_0 = \frac{\lambda}{\pi \alpha} = 147 \text{ } \mu\text{m}, \quad z_R = \frac{\pi w_0^2}{\lambda} = 6.4 \text{ cm.} \quad (2)$$

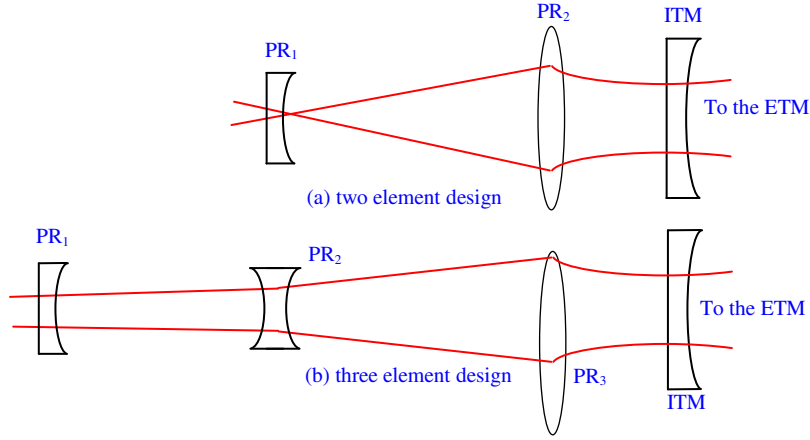


Fig. 2. a) One possibility to have a non-vanishing Gouy phase in the RCs is to focus the beam from the Input Test Mass (ITM) using one strong lens (PR_2) or curved mirror. Such a design creates a very small beam on PR_1 . The corresponding Rayleigh range would be very short and would make this design very sensitive to any ROC mismatches, b) The three element design allows to combine the fast beam expanding telescope formed by PR_3 and PR_2 with a distance between PR_1 and PR_2 where the spatial modes can gain the necessary Gouy phase to increase the transversal mode spacing.

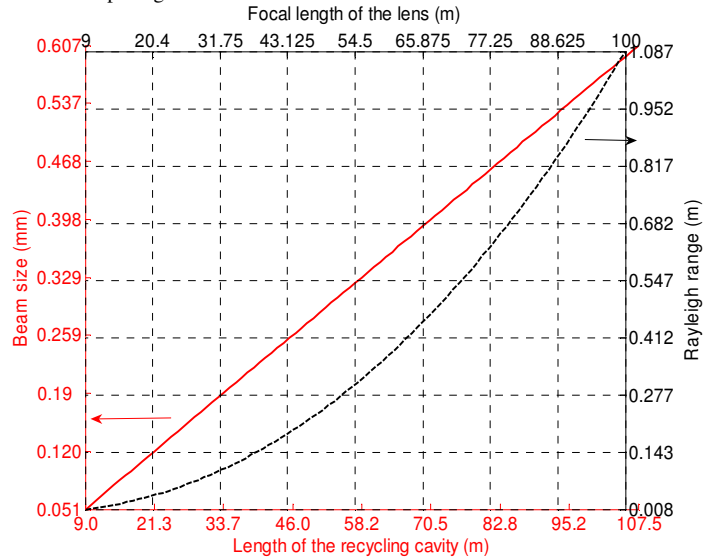


Fig. 3. The beam size (red curve, left axis) and Rayleigh range (black curve, right axis) for a two element RC as a function of focal length of the main lens and length of the RC. The length has to be rather long before the beam size reaches any reasonable value.

The recycling mirror PR_1 would have to be placed inside the Rayleigh range to have any appreciable Gouy phase or transversal mode spacing between the higher order modes. Such a

small beam size and Rayleigh range is not a reasonable option given the power which will be stored inside the PRC, the uncertainties in ROCs due to manufacturing errors and thermal lensing, and the additional requirements of matching the length of the RCs with the modulation frequencies. Even if the RCs would be folded inside the LIGO vacuum envelope to increase their length, the increase in Rayleigh range and beam size is rather slow. This is shown in Fig. 3 for a specific Gouy phase of $\pi/2$. The RC length has to increase to 100m to increase the waist size to $600\mu\text{m}$, still a rather small beam size and short Rayleigh range. An additional disadvantage would be that the sensing of alignment signals scales with the beam size and a small beam will reduce the alignment signals for this particular mirror significantly.

We decided to pursue a three element design which includes the beam expanding (in the PR arm) or beam compressing (in the SR arm) telescopes (see Fig. 2b). First the beam size is reduced by a strong lens or curved mirror (PR_3). A second lens or curved mirror (PR_2) is then placed at a position where the converging beam size is still a few mm in radius. This lens reduces the divergence angle to a value which corresponds to a waist size of a few mm or a Rayleigh range of a few ten meters matching up with the distances between the vacuum chambers in LIGO. In this design the spatial modes gain the required Gouy phase while they travel between PR_2 and PR_1 . The ROC of PR_1 is then chosen to match up with the received mode.

The final Gouy phase is essentially set by the focal length of PR_2 . For example, if the focal length ($f < 0$) of PR_2 is larger than the ROC of the phase front coming from PR_3 , the field will diverge before it ever reaches a waist. The Gouy phase would be close to 0. Decreasing the focal length further at one point will allow the beam to converge. However as long as the waist of this mode is still far outside the PR_1 and PR_2 part of the RCs, the Gouy phase will only increase slowly. But once the location of PR_1 is within the Rayleigh range of the new mode, the Gouy phase starts to increase significantly. However, if the focal length decreases further and the waist location is now closer and closer at PR_2 , the one way Gouy phase will reach π and the cavity will again be marginally stable. This is shown in Fig. 4 where we plot the Gouy phase and the spot size on PR_1 as a function of the ROC of PR_2 . Here we assume PR_3 ROC = 35.048m while the ROC of PR_1 will always be matched to the cavity mode.

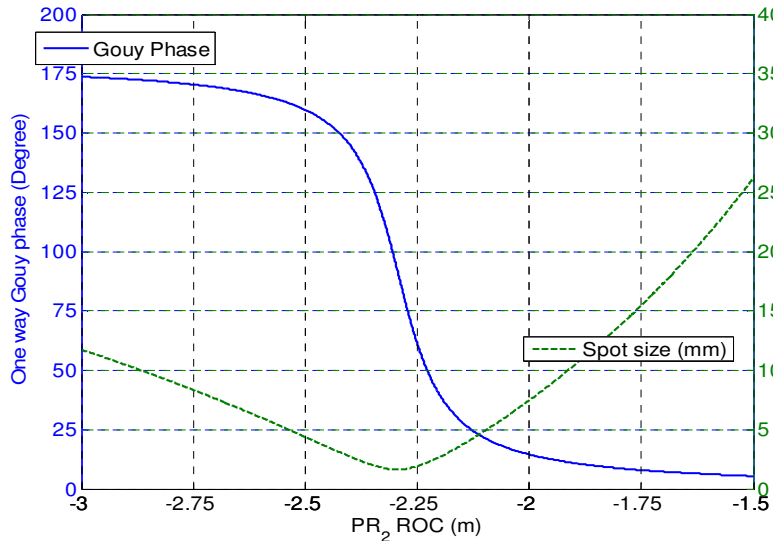


Fig. 4. The Gouy phase and beam size in a three element RC as a function of the ROC of the second element (PR_2). The minimum spot size is 1.6mm at a Gouy phase of 90° . Although small this beam size should allow to develop a reasonable alignment sensing scheme.

This design includes a rather fast and sensitive telescope between PR₃ and PR₂. In the following paragraphs we will discuss this in more detail using a preliminary design which assumes one-way Gouy phases of

$$\Psi_G^{PR} = 2.08 \text{ rad} \quad \text{and} \quad \Psi_G^{SR} = 0.51 \text{ rad} \quad (3)$$

inside the PRC and SRC [11,16]. These values evolved from preliminary optimization studies where we looked at the effects of the transversal mode spacing on alignment sensing, parametric instabilities, and higher order mode losses. These studies will be published later and the following results do not change significantly with the choice of the Gouy phases.

The current design parameters for the stable RCs are shown in Table 1. These design parameters are calculated using ABCD matrices and Gaussian modes to describe and propagate the laser field inside the interferometer.

Table 1. The current design parameters for stable PRC and stable SRC. R_i are the ROCs of the three mirrors PR_i or SR_i. L_{ij} are the distances between mirrors ij; I stands for the ITM mirror. All values in m.

Cavity	R ₁	R ₂	R ₃	L ₁₂	L ₂₃	L _{3I}
PR	8.95	-2.335	35.048	16.586	16.677	25.3404
SR	107.29	-2.155	35.048	16.586	16.677	25.3404

3. Requirements on mode matching

The carrier field will resonate in a fundamental Gaussian mode inside both arm cavities. The reflected carrier field interferes then at the beam splitter such that all the power is going back to the PRC. This cavity will build up the carrier to further enhance the amplitude of the carrier inside the arm cavities. The final build up in the arm cavities depends on the mode matching between the two cavities as well as other losses in the arm cavities and in the RCs such as contrast defects, absorption, scattering, and diffraction losses.

3.1 Power recycling cavity mode matching

For given losses inside the interferometer, the optimum build up is achieved when the entire interferometer as seen from the laser is impedance matched. This would require a transmissivity of the PRM of $T_{PR} = L_{RC} + 4L_{AC} / T_I$ where T_{PR} is the (power-) transmissivity of the PRM and T_I of the ITM. L_{RC} are the round-trip losses in the RC and L_{AC} the round-trip losses in the arm cavities. The carrier field in the arm cavity will then be:

$$E_{cav} \approx \frac{2 E_{in}}{t_I t_{PR}} = \frac{2 E_{in}}{\sqrt{L_{RC} T_I + 4 L_{AC}}}, \quad (4)$$

where $t_x = \sqrt{T_x}$. The design goal for the PRC is to reduce the losses such that the achievable build-up is limited by the arm cavity losses, i.e., $L_{RC} < 4L_{AC} / T_I$. Advanced LIGO designs carries a transmissivity of about 2.4% for the PRM, assumes round trip losses in the arm cavities of L_{AC} = 75ppm (factor two lower than in the current LIGO arm cavities), and a transmissivity of the ITM mirror of T_I = 1.4%. In that case, the effective losses in the RC caused by the arm cavity losses are about 2.1%. Consequently, the goal is to keep the roundtrip losses in the RC well below 1% and use a PRM with a transmissivity of about T_{PR} ≈ 2.4%. Note that this is not an extremely critical requirement for the PRC as losses in the interferometer which reduce the carrier power in the arm cavities can be compensated by increasing the laser power until the desired power level is again achieved. The main drawback of this approach would be the increase in scattered light or non-modematched light which circulates inside the interferometer.

3.2 Signal recycling cavity mode matching

The SRC is not impedance matched and the SRM mirror will have a much higher transmissivity of possibly even 20%. This reduces the effective signal loss inside the SRC for any given roundtrip loss as compared to the 'high Finesse' PRC. However, signal losses can not be compensated by increasing the laser power without changing the radiation pressure effects inside the arm cavities. The latter would also change the entire frequency response and dynamic behavior of the instrument.

4. Tolerance error in ROCs

Advanced LIGO has to take into account manufacturing tolerances in ROCs of all interferometer mirrors. Coupled cavities such as the RCs coupled to the arm cavities are intrinsically sensitive to spatial mode mismatches. The ROC of the input and end test masses of the arm cavity mirrors are about 2km. It is assumed that these ROCs can be manufactured with an accuracy of $\pm 0.5\%$ or $\pm 10\text{m}$. In this paper, we assume similar relative tolerances for all interferometer mirrors.

The effect of ROC mismatches in coupled cavity systems such as Advanced LIGO depends on the tuning of the various cavities and the details of the mismatch. For example, it is well known from initial LIGO that the spatial mode of the carrier inside the PRC is completely dominated by the arm cavity spatial mode. The reason is that the carrier is anti-resonant in the PRC alone and only builds-up because of the 180° phase shift caused by the arm cavities. On the other hand, the RF-sidebands used to control the longitudinal degrees of freedom resonate only inside the RCs and are not affected by the arm cavity eigenmode. Consequently, any mismatch between the RCs and the arm cavities will result in a degradation of the beat signals between these frequency components.

In contrast to this the SRC in Advanced LIGO will not be anti-resonant for the carrier. The SRC will be tuned to a particular frequency or even be resonant for the carrier (resonant sideband extraction). This will change the losses due to mode mismatch significantly. Quantifying the resulting losses and mode mismatched for all possible tunings is beyond the aim of this paper. Instead we quantify the mode matching and derive tolerances based on simple mode matching calculations where we ignore the changes in the spatial modes caused by the coupling of the cavities. This approach will in general overestimate the losses in the PRC while the losses in the SRC can be higher or lower depending on the tuning of the SRM and the frequency of the signal sidebands.

4. ROC Tolerance of PRC and SRC

The recycling mirrors PR_2 (SR_2) and PR_3 (SR_3) form a relatively fast telescope inside the power (signal) RC. Consequently, the spatial eigenmode inside the RCs is very sensitive to any ROC error. Comparatively, the remaining mirror, i.e., PR_1 (SR_1) has much relaxed ROC error tolerances. Figure 5 shows the mode matching between the RC eigenmode as seen by the RF sidebands and the arm cavity eigenmode. The white areas in the false color plots indicate regions where the nominal eigenmodes are unstable. Even a 0.1% increase in the ROCs of PR_3 and SR_3 will destabilize the spatial eigenmodes of the RF sidebands inside the RCs. Also a 0.3% decrease of ROCs will destabilize the spatial modes. This rather discouraging result appears to indicate that the stable cavity design is as sensitive to ROC errors as the current LIGO PRC.

In contrast to the current LIGO design, the new design allows to adjust the distance between the fast telescope mirrors. This allows stabilizing the spatial eigenmode of the RCs and regaining the mode matching. However, two boundary conditions have to be met. First, the overall length of the PRC and SRC has to be maintained to allow the fixed RF sidebands to build-up within the interferometer. Consequently, any change in the distance between the telescope mirrors has to be compensated by changes in the distances between PR_2 and PR_1 or SR_2 and SR_1 , respectively. Second, the range over which the mirrors can move is restricted by

the vacuum envelope and other in-vacuum components such as the Faraday isolator or beam paths in and out of the mode cleaner.

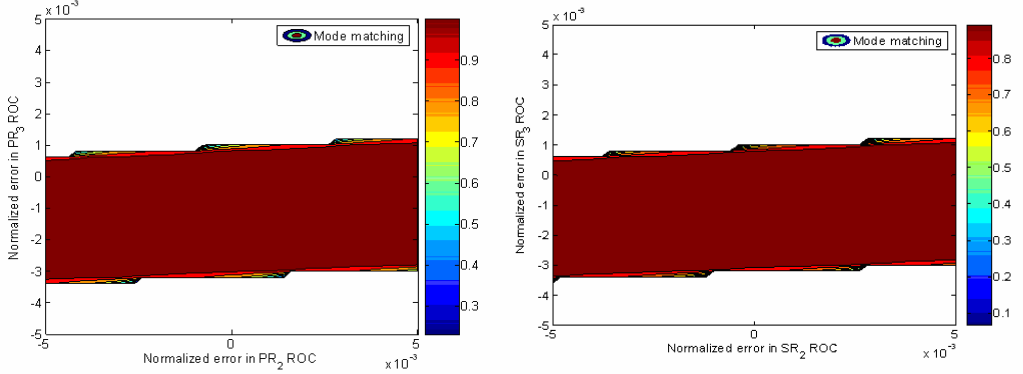


Figure 5: Left graph: The mode matching (in power) between the PRC and the arm cavity eigenmode as a function of the normalized errors in the two RC mirrors PR_2 and PR_3 . Right graph: The same graph for the SRC. The white areas are areas where the RCs are nominally unstable (g -factor > 1).

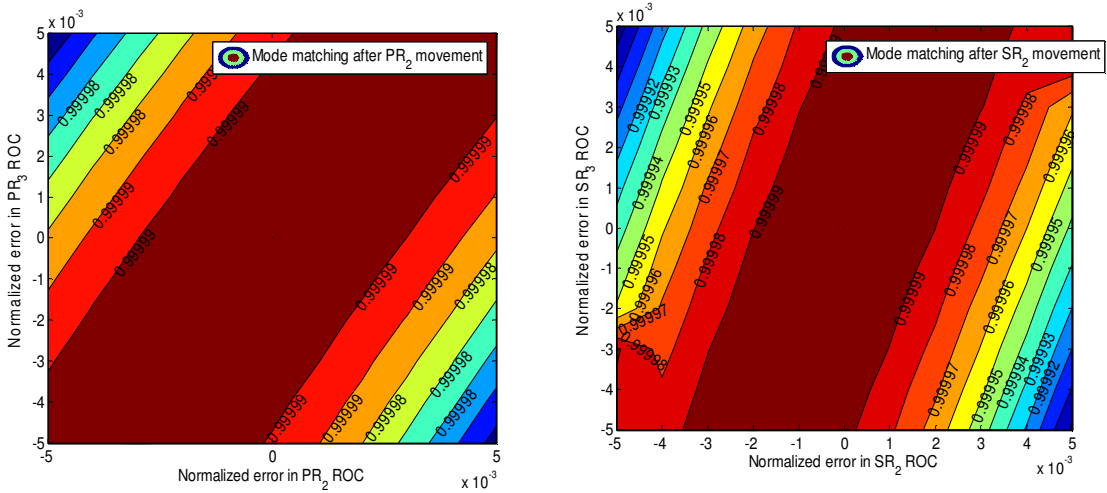


Figure 6: Left graph: The mode matching between the PRC and the arm cavity eigenmode as a function of the normalized errors in the two RC mirrors PR_2 and PR_3 after optimizing the distance between PR_2 and PR_3 and maintaining the overall length of the RC. Right graph: The same graph for the SRC.

The mode matching between the eigenmodes of the PRC and the arm cavities after optimizing the distances between the mirrors is shown in the left graph of Figure 6. The same result for the re-optimized SRC is shown in the right graph. Note that the color scales are completely different between the figures. Even in the worst case, we will be able to reduce the nominal mode mismatch to well below 100ppm, a level at which other losses such as diffraction losses, scatter, and absorption dominate. The required changes in the distances between the mirrors are in the order of the deviations in the ROCs of PR_3 and PR_2 or about ± 20 cm motion of PR_1 . The layout of the input optics for Advanced LIGO has to provide this range for PR_1 ; PR_2 has to move by approximately ± 10 cm on an optical table which is essentially empty.

In both cases, the round trip Gouy phases or the transversal mode spacing after re-optimizing the mode matching is again very close to the design values. Consequently, both RCs will always be stable and higher order modes will be non-resonant.

4.2 Tolerance in test mass ROCs

The ROCs of the test masses will be around $2\text{km}\pm 10\text{m}$. The tolerances in the ROCs will change the eigenmode inside the arm cavities and will reduce the mode matching between the RCs and the arm cavities. The left graph of Figure 7 shows the mode matching as a function of the ROCs of the two test masses without optimizing the distance between PR_2 and PR_3 . Note that the ranges for the ROCs are a factor two larger than the above mentioned tolerances. Even without any corrections in the mode matching telescope, the mode mismatch will stay below 1000ppm. Adjusting the distance between PR_2 and PR_3 while maintaining the RC length by moving also PR_1 by the appropriate amount allows to recover even these small differences. The SRC shows a similar behavior, any minor mismatch can be recovered by adjusting the telescope inside the SRC. The changes in the round trip Gouy phase are in all cases below 10^0 and higher order modes will again be non-resonant. It should be noted that the required tuning range for the SRC, the linewidth of the RCs, and the uncertainty in Gouy phase of the optimum mode matching will not allow to guarantee that all higher order modes are in all cases non resonant.

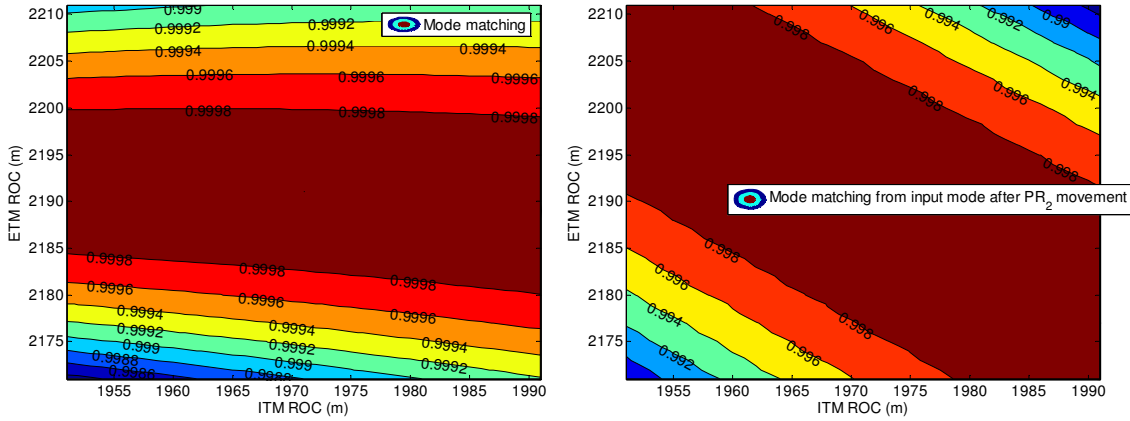


Figure 7: The mode matching (in power) between the RC and the arm cavity as a function of ITM and ETM ROC. The left graph shows the mode matching w/o length adjustments, the right graph shows the mode matching with length adjustments. The adjustments were made without changing the overall length of the RC and without changing the mode matching to the input mode.

However, adjusting the RCs will change the mode matching between the input beam coming from the input mode cleaner and the PRC or between the output mode cleaner and the SRC. The right graph in Figure 7 shows the degradation in this mode matching for the PRC if the telescope is adjusted to match the RC to the arm cavity. The loss stays below 1% even for the worst case scenario.

4.3 Compensation via Thermal Compensation System (TCS)

Note that Advanced LIGO will not rely entirely on manufacturer tolerances and our ability to optimize the distances between the RC mirrors to match the eigenmodes of the various cavities. In addition, Advanced LIGO will employ adaptive mode matching techniques known as the thermal compensation system (TCS) to correct any residual ROC mismatches [17]. The TCS uses CO_2 laser beams or ring heaters to heat up and shape the mirror surfaces and write appropriate thermal lenses into the substrates to optimize the mode matching actively. Although it has been shown that the TCS can correct ROC mismatches of up to 50m for km-scale ROCs; well above the tolerances of the mirrors, the TCS adds noise to the interferometer

and adjusting the mode matching passively as much as possible will reduce the amount of added noise significantly.

5 Summary

The PRC in the current LIGO detector consists essentially of flat mirrors and has a transversal mode spacing well below the linewidth of the cavity. Consequently, the spatial eigenmodes of the RF sidebands which are used to control all longitudinal and most angular degrees of freedom are not well confined. Only the installation of a thermal correction system allowed LIGO to reach its current design sensitivity. The next upgrade of LIGO, Advanced LIGO, will use power and signal recycling to enhance the carrier and the signal sidebands. In this paper we describe alternative designs for both RCs in which both cavities have a well defined spatial eigenmode and a transversal mode spacing which is well above the linewidth of the cavity.

We also discussed briefly the allowed mode matching losses between the RCs and the arm cavities. The main part of the paper shows that this new design is flexible enough and can be adjusted to easily accommodate ROC mismatches as long as the mismatches stay within the quoted manufacturing tolerances.

Acknowledgements

The authors want to acknowledge the support of the LIGO Science Collaboration. Especially the discussions with Hiro Yamamoto, Peter Fritschel, Mike Smith, Bill Kells, Luke Williams, Garilynn Bilingsley, Dennis Coyne, Volker Quetschke, David Reitze, and David Tanner were very helpful. This work was supported by the National Science Foundation under grant PHY-0354999.